High-Accuracy Pick-and-Place of Multiple Dies in Parallel Assisted by Capillary Self-Alignment

[1]Birgit Brandstätter, [1]Benedikt Auer, [1]Hannes Klingler, and [2]Sabine Scherbaum
[1]Besi Austria
Innstraße 16
Radfeld, 6241 Austria
Email: birgit.brandstaetter@besi.com
[2]Fraunhofer-Einrichtung für Mikrosysteme und Festkörper-Technologien EMFT
München, 80686 Germany

Abstract
Self-assembly of components driven by liquid surface tension is an attractive complement and even alternative to traditional high-accuracy pick-and-place as it offers high accuracy despite inaccurate robotic part placement. While capillary self-alignment through liquid solder is the standard technology for flip-chip processes, this work presents self-alignment of dies on wetted receptors on a temporary carrier: Low-viscosity liquid is jetted on each receptor where the liquid is contained through generation of hydrophilic and hydrophobic sections on the temporary carrier by plasma treatment. Deterministic die feeding by low-accuracy pick-and-place is conducted for single dies, as well as for batches of three dies and nine dies optimizing the equipment for best throughput to achieve both high accuracy and high productivity. The industry-ready and fully automated chip-to-wafer pick-and-place process is implemented into a fan-out wafer-level packaging production flow proving that self-alignment is capable of easing the stringent requirement for robotic alignment capability for pick-and-place systems in fan-out packaging for the single die-level step in this production chain. The self-alignment process is optimized, and failure modes such as poor liquid confinement, surface contamination, or excess force are identified and eliminated. Post-bond accuracy of <3 µm @ 3 σ at each point of the die is reached for dies of 3.1 mm x 3.1 mm in size. Using parallel die handling, high speeds of around 10 000 units per hour are made possible.

Key words
Advanced packaging, high accuracy, fan-out wafer-level packaging, manufacturing, pick-and-place, self-alignment.

I. Introduction
High-accuracy and high-speed pick-and-place enables advanced packaging processes, heterogeneous integration, and More-than-Moore roadmaps. High accuracy is essential for decreasing package size and high I/O count. High throughput allows for profitability and justifies manufacturability. However, increasing accuracy decreases assembly speed and vice versa, and equipment optimization always needs to balance this trade-off. Here, self-alignment driven by liquid surface tension drastically decreases the stringent requirement for robotic alignment capability for the pick-and-place equipment and thus allows the equipment to be optimized for best throughput [1]. Capillary self-alignment is the standard technology for flip-chip processes [2] exploiting the high surface tension of liquid solder and is widely used to electromechanically fix surface-mount components e.g. solder die-attach of power devices. In contrast, this work elaborates on self-alignment of dies on wetted hydrophilic receptors [3]– [5]. The receptors are designed to match the exact die size and geometry and are patterned lithographically on a temporary fan-out carrier. For the self-alignment process, the receptors are coated with a low-viscosity liquid. The pick-and-place equipment automatically deposits this liquid through non-contact, single-droplet jetting with accurate volume control. Die feeding is performed deterministically through pick-and-place. The fully automated chip-to-wafer pick-and-place process is further implemented into a fan-out wafer-level packaging (FOWLP) production flow [6]: The self-alignment-assisted pick-and-place is conducted face-up onto a temporary self-alignment carrier. In subsequent steps, a wafer-to-wafer bond onto the fan-out carrier is performed

together with a lift off from the self-alignment carrier, and the standard production flow of a chip-first face-down process is then completed, including molding and carrier removal.

This paper presents the industry-ready pick-and-place process flow for the single die-level step in this production chain using self-alignment to achieve both high-accuracy and high throughput in die assembly.

II. FOWLP though Self-Alignment

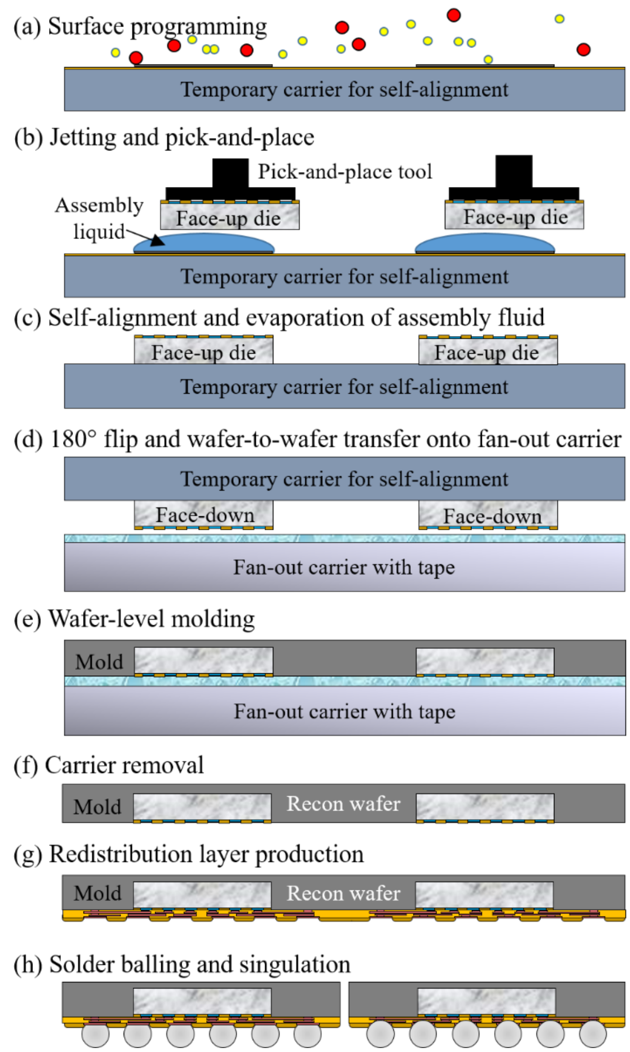

Fig. 1. Process flow for the FOWLP production including pick-and-place assisted by capillary self-alignment.

A. FOWLP Process Flow

Fig. 1 shows the process flow for FOWLP with pick-and-place assisted by self-alignment. The process steps are as follows: (a) The wetting properties of a temporary carrier wafer for self-alignment are programmed by a low-pressure carbon-tetrafluoride plasma-treatment: the metal areas become hydrophilic while the surrounding polyimide area becomes hydrophobic [3]. (b) After plasma treatment, assembly liquid is jetted onto the metal landing areas. Subsequently, thin dies are placed to float on the liquid. The weight of the die leads to the liquid wetting the full landing area. No exact pre-alignment is necessary, as long as the die is released to contact the liquid droplet. (c) Self-alignment of dies is driven by minimizing the liquid surface, given the matching size and geometry of die and receptor. The dies are fixed to the landing areas after all assembly liquid has evaporated. (d) The self-alignment carrier is flipped, and the dies are transferred to the fan-out carrier and thermal release tape. All further steps, thereby including molding (e), carrier removal (f), redistribution-layer patterning (g), and balling and singulation (h), correspond to the established FOWLP process flow.

B. Self-Alignment Material

The self-alignment carrier wafer is produced such that it has a polymer surface and lithographically patterned landing areas (aluminum) on top. The wafer is treated with a fluorine remote plasma process (CF_4 with 20% O_2) for two minutes. The metallic receptors turn hydrophilic while the surrounding polymeric material turns hydrophobic. Contact angles for the assembly liquid on the polymer rise to ~99° while the contact angle on the aluminum decreases to ~12° [7]. Thus, when jetting assembly liquid, the liquid spreads over the receptor and is confined by the surrounding hydrophobic area.

The assembly liquid used in the context of FOWLP ensures both the alignment of the dies to the landing area and a loss-free transfer process to the fan out carrier. Thus, the liquid formulation has to guarantee adhesion after die placement and must allow for easy release after the transfer process. In this work, the assembly liquid is chosen to comprise DI-water with an added water-soluble adhesive. This formulation is adapted to the adhesion of the thermal release transfer tape of the fan-out carrier.

Specific test material to prove the FOWLP process flow including self-alignment as outlined in Fig. 1 was designed and produced. Dies with 3.1 mm * 3.1 mm size and 150 µm thickness were used for all tests. The test dies have dedicated accuracy fiducials on the component backside to facilitate accurate post-bond accuracy measurements (Sec. F). A first batch of test material had Vernier structures and cutouts on two of the four die corners. For simplification, both were removed in a second batch of test material.

C. Single-Die Pick-and-Place

Pick-and-place was performed using the Datacon 2200 evo^{advanced}, a multi-module attach equipment with integrated jetter [8]. This industrial die bonder is a tried-and-tested platform with low cost-of-ownership and high-speed throughput.

Pick-and-place assisted by self-alignment comprises the following process steps: First, the bonder locates and ejects a die from a die wafer mounted on film frame. The flip tool picks up the die, flips it by 180° and transfers it to the bond tool. The substrate camera, which moves together with the bond tool, determines the position of a module on the substrate via image recognition. For the specific test material, a module is defined by a matrix of 3 x 3 bonding positions, therefore the module-adjust is done on every ninth bonding position. Next, the integrated jetting system dispenses a volume-controlled amount of assembly fluid onto the bonding position via a defined pattern of single dots (Sec. E).

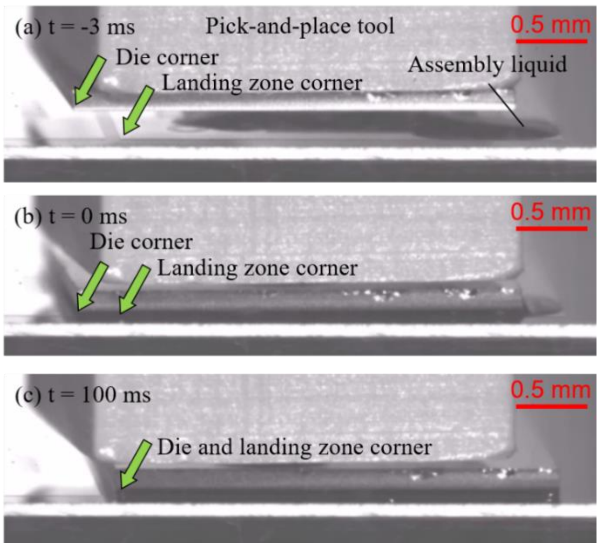

Fig. 2: High-speed camera images of the self-alignment process. (a) The bond head transports the 3.1 mm x 3.1 mm die to the receptor with a large initial offset (~300 µm). (b) The bond tool releases the die to float on the assembly liquid. (c) The die aligns to the receptor through surface minimization of the assembly liquid.

Subsequently, the bond head releases the die slightly above the bond position such that the die floats on top of the receptor. The die aligns through surface minimization of the assembly liquid within ~100 ms (Fig. 2). Finally, the substrate camera inspects the bonded die and evaluates the placement accuracy. While the equipment continues with the pick-and-place cycle for the following dies, the assembly liquid evaporates slowly and the die attaches to the receptor. It is worth noting that the capillary retention force increases as the liquid lubricating film evaporates, until film break-up.

In the process tests, a state-of-the-art high-speed camera and optics were utilized to monitor and optimize the process. The pick-and-place tests show that the self-alignment process is insensitive to placement offsets of more than several hundred µm, purposely induced to study process stability, confirming prior results in literature such as [9], [10]. The process window for die release height is determined to be around 200 µm, and the die did not necessarily touch the liquid upon release: Releasing the die too high above the substrate leads to a long free fall of the die, which in turn can lead to splashing or horizontal die shift. A low release height squeezes out the assembly liquid, leading to spill over onto the hydrophobic area and compromising the final die placement. This process window for release height depends on the initial thickness of the liquid droplet (in this work approximately 70 µm) and on the size and geometry of the receptor.

D. Multi-Die Pick-and-Place

Pick-and-place tests were conducted in two stages. The first bonds were performed sequentially, one die after another as described in Section C above. In the second test, the bonder ejected, transferred, and bonded multiple dies at once in order to increase throughput. Test for bonding multiple dies in parallel were done with three dies and nine dies, respectively.

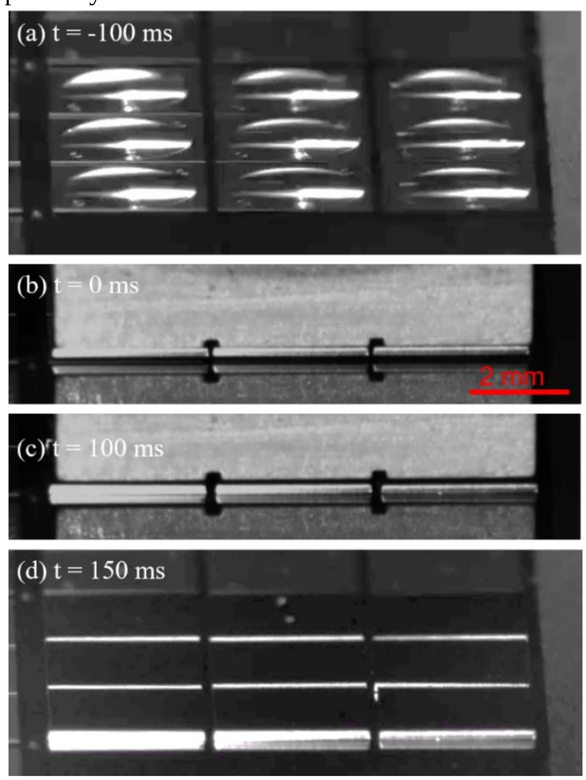

Fig. 3: High-speed camera images of nine dies (each 3.1 mm x 3.1 mm) bonded simultaneously using capillary self-alignment.

The sequence for bonding multiple dies per bond cycle was as follows: Dies were ejected collectively and picked up by the flip tool. The flip tool rotated all dies upward and transferred them to the bond tool. Next, the equipment jetted the assembly liquid sequentially on all relevant bonding positions and placed all dies in parallel. The floating dies self-aligned to the exact bond position. Fig. 3 shows high-speed camera images of (a) nine bond positions prepared with assembly liquid, (b) nine dies on the bond tool just before the release (c) the dies floating and already aligned to the bond position, and (d) after the bond head left the module position for all nine dies.

II. Experimental Results and Discussion

E. Process Optimization

The die attach equipment employs a jetter with a nozzle of Ø = 100 µm to jet small volumes of liquid with the necessary high speed and mass precision. Depending on this nozzle size, volumes down to the ~1 µg can be jetted reliably. A mass repeatability of 5% is reached independent of the nozzle size. Dispensed liquid volume and the distribution of the assembly liquid over the receptor area are critical for the self-alignment process. Insufficient liquid does not fill the full receptor even after releasing the die, and thus, the die cannot self-align due to friction. Excess liquid leads to overflow beyond the receptor, and again makes self-alignment unsuccessful. Tests show that the die squeezes out any excess liquid. The optimum dispensing mass for the test material used in this work was determined to be between 0.4 mg and 0.6 mg. For a given receptor area and geometry, this process window depends on the die's weight (depending on the die thickness) becoming smaller for thicker dies. Additionally, the process is limited to dies that are able to float on water through surface tension forces.

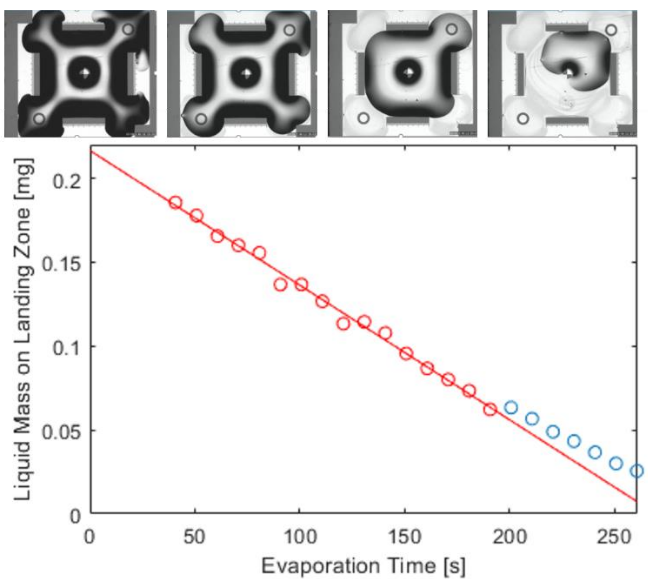

Fig. 4: Time dependence of liquid mass jetted on the receptors. Until ~200 s the evaporation is linear. These data (red) are used in a linear fit. The substrate camera images on the top show the liquid distribution over time.

To determine acceptable process times between liquid jetting and die release, a measurement of the evaporation rate of the liquid on the receptor was undertaken using a precision scale to measure liquid mass a function of time. Fig. 4 shows the evaporation time of a mass of a 0.22 mg of assembly liquid spread over the 9.6 mm^2 receptor. After 250 s, the liquid has almost completely evaporated. Considering the process window of liquid volumes between 0.4 mg to 0.6 mg, jetting volumes of 0.6 mg allow for die placements of maximally 4 minutes after jetting. Thus, the time between jetting and bonding must not change significantly and a bond has to be aborted if an unexpected delay occurs after jetting. Equipment settings were subsequently set to account for such delays and trigger corrective actions.

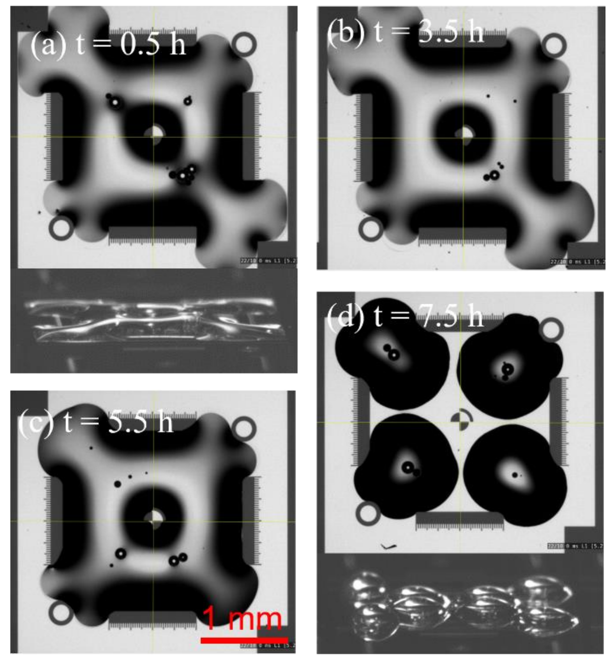

Fig. 5: Substrate camera images and photographs from the side of the receptors prepared with assembly liquid with different times between plasma activation and liquid deposition.

It is further noteworthy that the hydrophilic / hydrophobic programming of the plasma-treated surface loses its properties over time. Fig. 5 shows the distribution of jetted assembly liquid as a function of time passed after plasma treatment: The liquid spreads well for around 4 h after plasma treatment, while wetting uniformity deteriorates after that as evidenced by liquid film rupture.

For bonding multiple dies simultaneously, the blow-off air pressure, which releases the die from the bond head, is identified as a main challenge. The air blowing off the center die streams out over the adjacent dies and leads to an outward force. For nine dies even a small blow-off pressure leads to a significant outward force, pushing the floating dies away from the ideal bond position. However, too little blow off pressure hinders the ventilation of the vacuum channel and the dies end up staying on the bond tool. As a solution, an additional throttle is employed to ventilate the chip vacuum channel, such that the vacuum is strong enough to pick up the dies from the flipper and still able to release the dies in a reasonable time.

After process optimization for liquid mass and blow-off parameters, surface contamination by foreign material is identified as the main cause of decreased alignment accuracy. Conducting tests outside a back-end cleanroom environment leads to large dust particles (~100 µm) accumulating on the test substrate. Individual bond positions were then identified where self-alignment was unsuccessful with offsets up to hundred µm or more. Such bond sites showed visible dust particles between substrate and die by infrared inspection (Fig. 6).

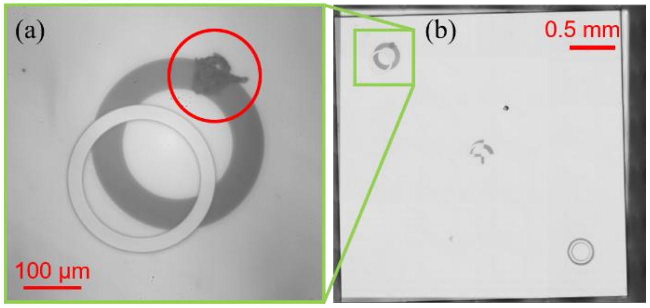

Fig. 6 (a) IR microscope image of visible contamination close to the upper left fiducial. (b) Stitched IR microscope image of die and substrate. The offset of the upper left fiducial is Δx = 61 µm and Δy = -59 µm while the offset of the lower right fiducial is Δx = 3 µm and Δy = 1 µm.

F. Accuracy Measurements

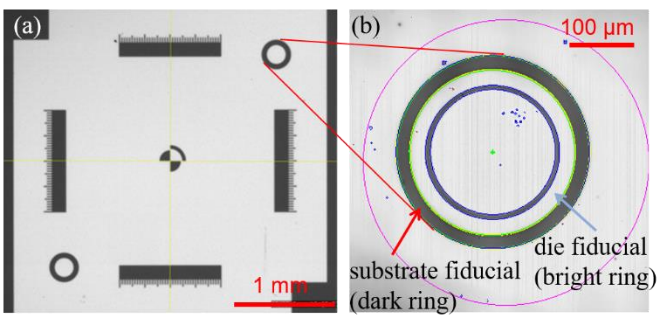

Fig. 7 (a) Substrate camera image of the component position on the carrier wafer. (b) IR microscope image and search results for a substrate fiducial (dark ring) and die fiducial (bright ring) on top.

The post bond analysis was performed using the bonding equipment's substrate camera as well as an external infrared (IR) wavelength automated microscope. The substrate camera quickly identifies poor quality of die edges, squeeze-outs of the adhesive liquid or large offsets while the IR measurement at infrared wavelength above 1200 nm allows for precision data collection of post-bond accuracy data looking through the silicon chip and making component and substrate fiducials visible. The automatic IR microscope was used for IR image acquisition. Besi's vision toolbox processed these images to perform ultra-accurate position measurements. Through pixel averaging, the measurement uncertainty for a circle center search using this vision system was determined to be ~10 nm @ 3 σ [11].

Fig. 7 (b) shows an IR microscope image of a bonded component picturing component fiducial and substrate fiducial acquired through the thin silicon chip. The image processing software was set to detect outer substrate-fiducial circle and the outer component-fiducial circle and it calculates their circle center offsets. The two substrate fiducials Fig. 7 (a) and the two die fiducials were used to calculate the x-, and y- placement offset at the die center as well as the component rotation (θ).

G. Accuracy and Throughput Results

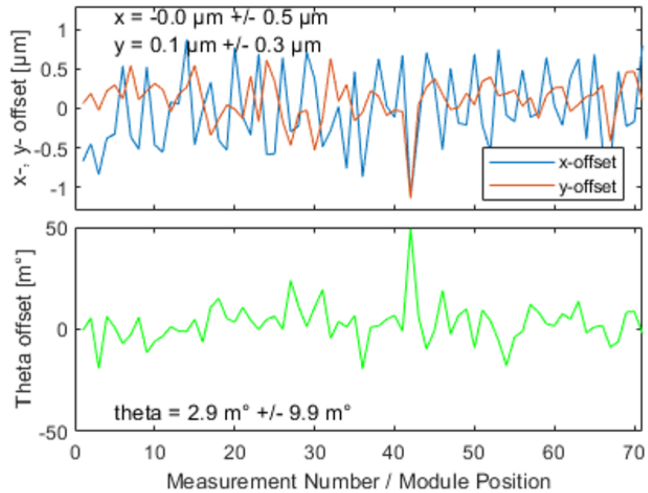

Fig. 8 x-, y-, and θ-accuracy for self-alignment tests of three dies bonded simultaneously. Standard deviations are given in 1 σ.

Accuracy and throughput data were collected for single-die self-alignment as well as for mutli-die self-alignment with three and nine dies, respectively. Fig. 8 shows x- and y-placement accuracy data and component rotation for self-alignment-assisted pick-and-place tests done by bonding three dies simultaneously. A total of 72 dies were bonded for this dataset.

Table 1. Pick-and-place results comparing conventional pick and place to self-alignment of single-die and multi-die. Standard deviations are given in 3 σ.

	Conventional pick & place	* Single-die self-alignment	** Multi-die self-alignment	** Multi-die self-alignment
Dies per bond-cycle	1	1	3	9
x–accuracy [µm]	0 ± 3	0.1 ± 3.9	0 ± 1.5	0 ± 2.3
y–accuracy [µm]	0 ± 3	1.2 ± 3	0.1 ± 0.8	0.2 ± 2.4
θ–accuracy [m°]	0 ± 70	-8.9 ± 111	3 ± 30	1 ± 75
Cycle time [s]	1.2	1.82	2.25	3.35
Throughput [UPH]	3000	2000	4800	9700

* old design and diced by grinding
** new design and singulated by plasma dicing

Table 1 shows the accuracy and throughput results for all process tests: single-die self-alignment and multi-die self-alignment with three and nine dies, respectively, and compares the performance of self-alignment with that of conventional pick-and-place.

Placement accuracy was on the order of 3 µm @ 3 σ for self-aligned dies, which compares well with the standard robotic alignment accuracy. The material used for single-die self-alignment was singulated through dicing by grinding, producing poorly defined die edges as compared to the material used for multi-die self-alignment, which was singulated by plasma dicing. Thus, as expected [1], the single-die self-alignment data shows larger systematic errors and slightly higher standard deviations than the multi-die self-alignment data. Process tests showed that current alignment accuracy was still limited by limited cleanliness of the test environment and higher accuracies might still be possible in a stable cleanroom environment.

Throughput decreased slightly for single-die self-alignment compared to conventional pick-and-place due to the added step of jetting. However, for multi-die self-alignment throughput drastically increases. The bond cycle for bonding three dies took 2.25 s, which equals a throughput of 4800 units per hour (UPH). Bonding nine dies at the same time leads to a bond cycle time of 3.35 s and a UPH of 9700. Moreover, such collective bonding has much potential to be accelerated even further e.g. by increasing jetting throughput through parallel jetting or stamping of assembly liquid and by further optimizing ejection of multiple dies.

III. Conclusion

A die-to-wafer pick-and-place process using capillary self-alignment was successfully transferred to an industrially-used die bonder proving that capillary self-alignment is applicable in a high-volume manufacturing. The automated self-alignment process was optimized and failure modes such as poor liquid confinement or large blow-off pressure were identified and eliminated. Tests showed that the bonding process needed precise jetting capability, accurate process timing, and appropriate cleanliness of a standard back-end cleanroom. Furthermore, plasma dicing proved advantageous for placement accuracy as compared to dicing by grinding. Developing multi-die self-alignment increased throughput and highlighted the process as an industrially competitive and applicable solution.

High-accuracy post-bond accuracy data were acquired by IR microscopy, and a self-alignment accuracy of <3 µm @ 3 σ at each point of the die was achieved for dies of 3.1 mm x 3.1 mm in size when bonding nine dies at the same time. Using parallel die handling of nine dies, high speeds of almost 10.000 UPH were made possible with potential for further speed gain through parallel jetting and optimization of ejection speed for ejecting multiple dies in parallel.

The process was implemented in a FOWLP production flow together with industrial partners such as EVG and Amkor Technology Portugal.

Acknowledgment

This work is part of the EuroPAT-MASIP project funded by the Austrian Funding Agency (FFG) under grant number 858948 and ECSEL Joint Undertaking under grant number H2020-ECSEL-2016-IA-737497.

The authors thank Amkor Technology Portugal for molding and carrier removal and EVG for wafer-wafer bonding and lift off, as well as Plasma-Therm for plasma dicing of test dies. The authors further thank Dr. Massimo Mastrangeli and Dr. Hannes Rieser for discussion and input.

References

[1] M. Mastrangeli, Q. Zhou, V. Sariola and P. Lambert, "Surface tension-driven self-alignment," *Soft Matter,* vol. 13, no. 2, pp. 304-327, 2017.

[2] L. F. Miller, "Controlled collapse reflow chip joining," *IBM Journal of Research and Development,* vol. 13, no. 3, pp. 239-250, 1969.

[3] K. Bock, S. Scherbaum, E. Yacoub-George and C. Landesberger, "Selective one-step plasma patterning process for fluidic self-assembly of silicon chips," in *Electronic Components and Technology Conference,* 2008.

[4] V. Sariola, M. Jääskeläinen and Q. Zhou, "Hybrid microassembly combining robotics and water droplet self-alignment," *IEEE Transaction on Robotics,* vol. 26, no. 6, pp. 965 - 977, 2010.

[5] T. Fukushima, J. Bea, H. Kino, C. Nagai, M. Murugesan, H. Hashiguchi, et al., "Reconfigured-Wafer-to-Wafer 3-D Integration Using Parallel Self-Assembly of Chips With Cu-SnAg Microbumps and a Nonconductive Film," *IEEE Transactions on Electron Devices,* vol. 61, no. 2, pp. 533-539, 2014.

[6] S. Scherbaum, C. Landesberger, B. Auer, H. Klingler, B. Brandstätter, E. Brandl and J. Bravin, "Toward improved FOWLP manufacturing by using self-alignment process," in *Smart Systems Integration; 13th International Conference and Exhibition on Integration Issues of Miniaturizes Systems*, Barcelona, 2019.

[7] C. Landesberger, S. Scherbaum, J. Weber, K. Bock, M. Hiroshima and B. Oberhofer, "Plasma dicing enables high accuracy self-alignment of thin silicon dies for 3D-device-integration," in *IEEE 2012 4th Electronic System-Integration Technology Conference (ESTC)*, 2012.

[8] Besi, "besi.com," 2021. [Online]. Available: https://www.besi.com/products-technology/product-details/product/datacon-2200-evo-advanced/. [Accessed 11 08 2021].

[9] Q. Zhou, V. Liimatainen and I. Routa, "Microsystem integration using hybrid microassembly," in *Proceedings of the 5th Electronics System-integration Technology Conference (ESTC),* Helsinki, 2014.

[10] V. Liimatainen, M. Kharboutly, D. Rostoucher and M. Gauthier, "Capillary self-alignment assisted hybrid robotic Handling for Ultra-Thin Die Stacking," in *IEEE International Conference on Robotics and Automation (ICRA),* FInland, 2013.

[11] B. Brandstätter, D. Aschenwald, B. Auer, N. Bilewicz, R. Boomsma, et al., "High-speed ultra-accurate direct C2W bonding," in *70th Electronic Components and Technology Conference (ECTC)*, Virtual Event, 2020.